Microscopic versus Macroscopic Glass Transition(s) in Blends of Industrial Interest

Numera Shafqat[1,2*], *Angel* Alegría[1,3], *Nicolas* Malicki[2], *Séverin* Dronet[2], *Lucile* Mangin-Thro[4], *Bernhard* Frick[4], *Juan* Colmenero[1,3,5], and *Arantxa* Arbe[1]

[1]Centro de Física de Materiales (CFM) (CSIC-UPV/EHU) - Materials Physics Center (MPC), San Sebastián, Spain
[2]Manufacture Francaise des Pneumatiques MICHELIN, Clermont-Ferrand, France
[3]Departamento de Polímeros y Materiales Avanzados: Física, Química y Tecnología, UPV/EHU, San Sebastián, Spain
[4]Institut Laue-Langevin, Grenoble, France
[5]Donostia International Physics Center (DIPC), San Sebastián, Spain

Abstract. We investigate by neutron scattering and calorimetry a mixture of styrene-butadiene rubber (SBR) and a commercial resin. The neat materials present a large dynamic contrast, having SBR a much lower glass-transition temperature than the resin. The focus is to exploit neutron scattering selectivity in an isotopically labelled sample where deuterated SBR is the majority component. This direct insight into the resin atomic motions within the mixture allows determining the 'microscopic' glass transition of the resin in the presence of the a priori much more mobile SBR. This transition takes place in the vicinity of the initial calorimetric glass transition temperature, mainly dictated by the majority component.

1 Introduction

Polymeric mixtures based on styrene-butadiene rubber (SBR) matrices are of high interest in tyre industry. Mixing components with markedly different microscopic mobility (and thereby showing a large difference in their glass-transition temperature (T_g) values) provides a very versatile tool to obtain materials with desired end-use properties. In addition to this applied motivation, the study of mixtures based on systems with strong dynamic asymmetry –i. e., presenting a large difference in the characteristic times of the segmental (α)-relaxation-- has attracted great academic interest in the past years [1].

Frequent experimental observations in polymer blends comprise (i) very broad relaxation responses (much broader than in the neat components) and (ii) distinct characteristic times associated to each of the components, even in thermodynamically miscible blends. It is by now well established that these phenomenological findings can be traced back to two major ingredients: concentration fluctuations which lead to the observed broadening of the measured response functions and self-concentration which causes a distinct dynamical response of the components [1-8]. The self-concentration concept refers to the fact that the local concentration around a given segment is always enhanced with respect to the average (macroscopic) concentration due to chain connectivity. We note that experimental investigations on blends dynamics become difficult due to the need of applying selective techniques allowing to isolate the component dynamics in the mixture, in order to determine their mutual influence upon blending. Therefore, thorough investigations resolving the dynamics of both components are scarce. Most studies involve calorimetric techniques as a first approach to the overall macroscopic characterization of blends' dynamics. In a calorimetry experiment, the effect of blending is observed as a broad feature, leading to a smooth variation of the specific heat over a temperature region between the T_gs of the pure components. If the dynamic asymmetry of the two components is extremely large –as it is the case of e. g. polyethylene oxide (PEO) and poly(methyl methacrylate) (PMMA)– the presence of two distinct contributions to the specific heat step associated to each of the components can be resolved [1,9-11]. However, this is not always possible. In general, an average T_g is determined for the blend from the inflection point of the heat capacity, that is usually considered as the representative glass-transition temperature of the mixture.

The question of the dynamical behaviour in dynamically asymmetric mixtures becomes even more intricate if we consider in addition compositionally asymmetric systems, i. e., mixtures markedly rich in one of the components. In the case of blends where the high-T_g component is the majority one, interesting confinement effects have been reported for the fast minority component. This was the case of the very flexible PEO chains in PMMA [12], poly(vinyl acetate) [13] (PVAc) or polyethersulfone (PES) [14] rigid matrices, or poly(vinyl methyl ether) in polystyrene (PS) [15]. In the present work we face the opposite situation,

* Corresponding author: nshafqat001@ikasle.ehu.eus

considering a mixture where the high-T_g component is the minority one. Our aim is to determine 'microscopically' the vitrification temperature of the minority component, and compare it with the glass transition of the system as determined by calorimetry.

The system here investigated is a binary mixture of industrial interest, composed by SBR as low-T_g component and a commercial resin as high-T_g component. The technique chosen to isolate the dynamics of the latter component and determine its 'microscopic glass transition' is neutron scattering, combined with isotopic (H/D) labelling. This is an ideal tool to provide direct insight into the atomic (in particular, H) motions of a given component in a complex system, if the rest of the material is deuterated. Therefore, to be sensitive to the dynamics of the resin in the mixture, we have investigated a sample where SBR is deuterated. The inspection of the thermal evolution of the scattered intensity has allowed us to discern the 'microscopic effective' T_g of this resin component within the blend. This is compared with the calorimetric results on the same sample. In this way, we can directly compare the 'microscopic' T_g of the resin component as determined by neutron scattering with the 'macroscopic' T_g observed by calorimetry on the whole system. The same kind of study is performed on the pure resin material, as reference.

2 Experimental

Samples were blends of a commercial polylimonene resin (M_n= 374 g/mol and PDI = 2.21) and deuterated SBR (M_n= 56400 g/mol and PDI = 1.40; styrene content: 19%, 1,2-butadiene content: 49.9%) synthesized in the laboratories of Michelin, following a similar procedure as described in Ref. [16].

Differential Scanning Calorimetry (DSC) measurements were carried out on samples of approximately 10 mg placed in aluminum pans using a Q2000 TA instrument. A liquid Nitrogen Cooling System (LNCS) was used with 25 ml/min helium flow rate. Data were acquired during cooling at 3 K/min. Temperature-modulated experiments (MDSC) were performed using a sinusoidal variation of 0.5 K amplitude and 60 s period.

The elastic fixed window scans (EFWS) were carried out by the IN16B backscattering spectrometer at the ILL [17] with a wavelength λ of 6.271Å, covering a scattering vector range $0.2 \leq Q \leq 1.9$Å^{-1}. The energy resolution of IN16B was 0.75μeV. The intensity scattered with energy transfer of 2μeV was also recorded during the heating scans (from 2 to 320 K, with a rate of 2 K/min). This maximum temperature was limited by beam time availability, but is above the glass-transition of the two neat components, being thus enough for the purpose of the current investigation. The blend sample investigated contained a weight fraction of dSBR w_{SBR}=0.80. Experiments on a pure resin sample were conducted as reference.

Whereas the mentioned isotope labelling strongly reduces the incoherent scattering of the deuterated component, it does not completely cancel its contribution, being now of mainly coherent nature. Therefore it is important to determine the Q-dependence of the coherent and incoherent scattering contributions as explained later. This is possible by exploiting polarization analysis. Experiments by the D7 instrument [17] at the ILL allowed accessing the ratio between coherent and incoherent differential scattering cross sections of the blend sample investigated by IN16B. With λ = 4.88 Å, a Q-range from 0.13 to 2.46 Å^{-1} was covered. In addition, we investigated blends with w_{SBR} = 0.50 and w_{SBR} = 0.15, as well as the pure dSBR sample. Experiments were carried out at 300 K. The thicknesses of the samples investigated by neutron scattering were chosen such that a transmission of about 90% was expected. They were filling flat aluminum sample holders and placed at 135° with respect to the incident beam.

3 Results and Discussion

The results on the reversible part of the heat capacity C_p^{rev}corresponding to the neat polymers and the blend with w_{SBR}=0.80 composition are presented in Fig. 1. The glass transition manifests as a jump in this function, and the value of T_g is commonly taken as the inflection point of C_p^{rev}. To give account for the broadening of this transition, the construction illustrated in this figure for the case of the blend results is usually made. For this sample, we deduce a value of T_g = 240 K, with initial and final glass-transition temperature values of $T_i = 235$ and $T_f = 244$ K respectively (see the arrows). The temperature-derivative of C_p^{rev} is also included in this figure for the three samples (empty symbols). The glass transition is reflected as a peak in this function, where the position of the maximum corresponds to the inflection point of C_p^{rev} and thus directly gives the value of T_g as usually defined. This function also reflects very clearly the width of the glass transition process and may allow resolving multiple transitions, if present in the sample [18,19]. In Fig. 1 we can observe that the glass transition process in the resin occurs at much higher temperatures than in the dSBR sample. This qualifies the blends of these two systems as dynamically asymmetric mixtures. In addition, we find that the glass-transition process in the resin spans over a much wider temperature interval than in dSBR. This feature can be attributed to the large polydispersity of the resin.

Blends with different compositions were characterized by DSC and the results regarding the location and width of the glass transition are compiled in Fig. 2. As can be seen, the usually invoked Fox equation

$$\frac{1}{T_g} = \frac{\varphi_{SBR}}{T_g^{SBR}} + \frac{(1-\varphi_{SBR})}{T_g^{resin}} \qquad (1)$$

where φ_{SBR} is the concentration of the SBR component and T_g^{SBR} and T_g^{resin} the T_g-values of the pure materials,

does not describe the concentration dependence of the average glass-transition temperature in these blends. It particularly fails in the range of concentrations in the SBR-poor side. The more flexible equation proposed by Gordon and Taylor [20]:

$$T_g = \frac{(1-\varphi_{SBR})T_g^{resin} + k_{GT}\varphi_{SBR}T_g^{SBR}}{1-\varphi_{SBR}+k_{GT}\varphi_{SBR}} \qquad (2)$$

actually describes the results with a much better accuracy. The value deduced for the parameter k_{GT}, that is related with the density and the increment of the isobaric expansivity at T_g of each component, is 2.36.

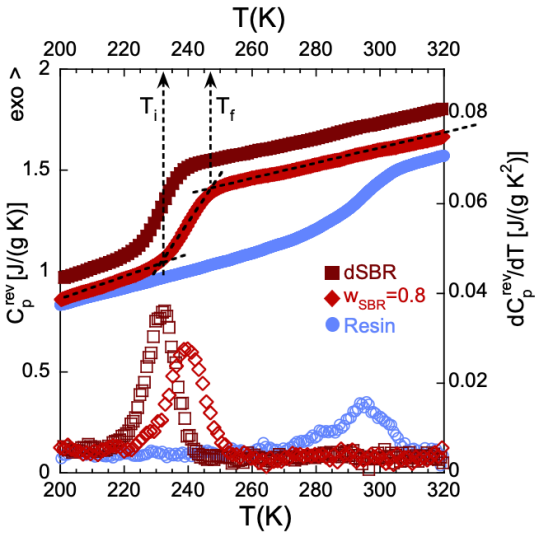

Fig. 1. Results obtained by modulated DSC on the pure components and the blend with 0.80 dSBR weight fraction: reversible part of the specific heat (filled symbols) and its temperature derivative (sign changed, empty symbols). Dotted arrows show, for the blend case, the usual construction to determine the initial and final glass-transition temperature values.

On the other hand, the width of the transition strongly increases with resin concentration. This finding could be attributed to either the persistence of a high degree of dynamic heterogeneity in the mixtures or to the intrinsic pronounced width of the glass-transition process in the resin (or to both factors). We note that at high SBR concentrations –as it is the case on which we are currently interested—the width of the transition is rather small, almost comparable to that observed for the neat dSBR sample.

Now we move to the neutron scattering results. The intensity scattered by a given sample has both, coherent and incoherent contributions [21]. In our investigation we are interested in the incoherent contribution arising mainly from the hydrogens in the protonated component of the blend. Usually this contribution is overwhelming due to the huge incoherent scattering cross section of H, compared with the rest of the scattering cross sections of the nuclei involved in the sample. However, if the composition of the sample is rich in the deuterated component –as it is our case—, since in D the coherent scattering cross section is higher than the incoherent one, the coherent contribution might present non-negligible values in some Q-regions. To determine the Q-range where the intensity scattered is less contaminated by coherent contributions we examined the D7 results. The measured ratio between coherent and incoherent differential scattering cross sections is shown in Fig. 3 for blends of different compositions including the particular one of w_{SBR}=0.80 on which we have focused our study. The figure also shows this magnitude for the pure dSBR blend. For the pure resin –not measured by D7— this ratio is expected to be below 10%. With increasing content of dSBR, the coherent fraction increases. In particular, an important coherent contribution is observed for the blends in the range around 1—1.2 Å^{-1}, reflecting the structure factor peak associated to the short-range order in these polymeric systems. Even more important, especially for the samples with high dSBR contents, is the pronounced increase of the coherent scattering at low Q-values, due to fluctuations of concentration in the mixtures [6,22]. Thus, if we want to minimize the effects of coherent contributions in our temperature scan results, we have to focus on Q-regions close to the minima: $Q \approx 0.7$ Å^{-1} and above ≈ 1.6 Å^{-1} in the case of the blend with w_{SBR}=0.80 (see Fig. 3).

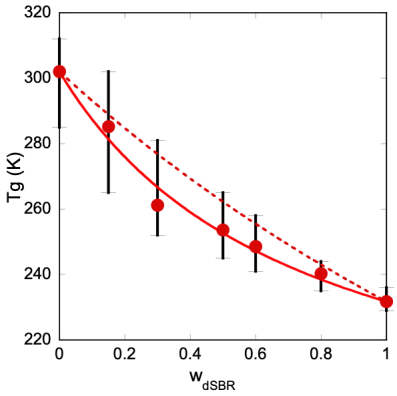

Fig. 2. Composition dependence of the glass-transition temperature T_g (inflection point of the specific heat). Error bars span between the of T_i and T_f determined by DSC. Dashed line shows the Fox prediction, and solid line the Gordon-Taylor description.

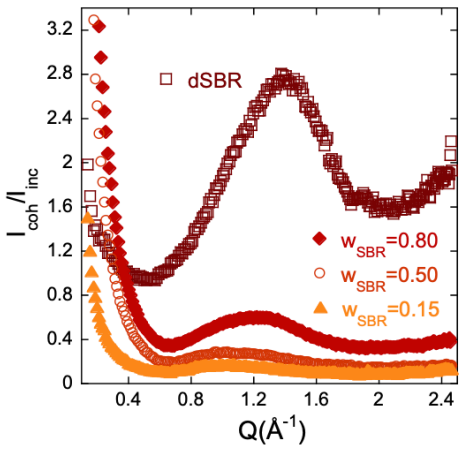

Fig. 3. Ratio between the coherent and incoherent differential scattering cross-sections determined by diffraction with polarization analysis (D7) on the pure dSBR system and blend samples with different compositions.

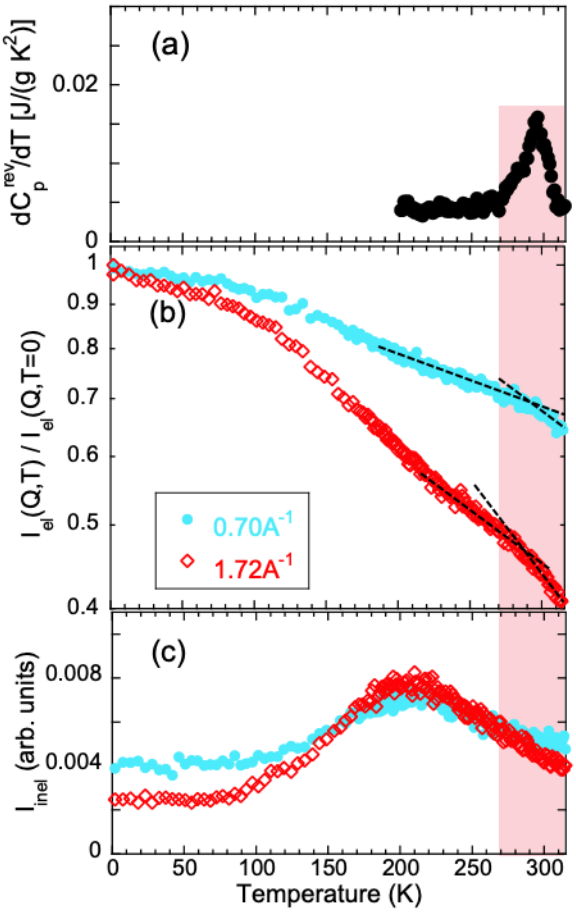

Fig. 4. Temperature dependence of results on the pure resin: (a) temperature derivative of the specific heat; (b) elastic intensity normalized to its extrapolated value at T=0; (c) inelastic intensity at 2μeV. Neutron scattering results correspond to the two Q-values indicated. Red area covers the calorimetric glass-transition region.

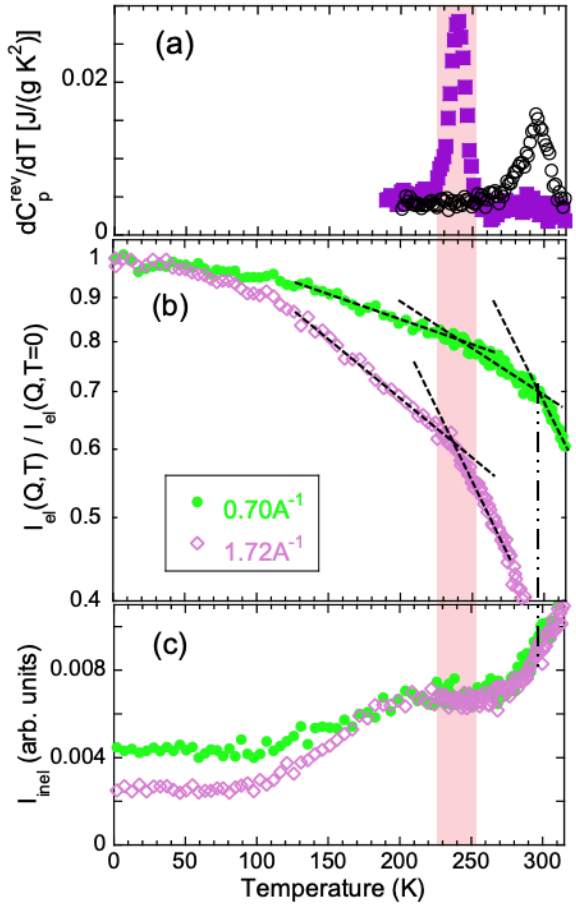

Fig. 5. Temperature dependence of results on the blend with 0.20 resin weight fraction in deuterated SBR: (a) temperature derivative of the specific heat; (b) elastic intensity normalized to its extrapolated value at T=0; (c) inelastic intensity at 2μeV. Neutron scattering results correspond to the two Q-values indicated. Red area covers the calorimetric glass-transition region.

Guided by the D7 results, we have focused our attention on the IN16B data collected at $Q = 0.70$ Å^{-1} and $Q = 1.72$ Å^{-1}. They can be seen in Fig. 4 for the case of the pure resin (reference system) and in Fig. 5 for the blend. These results are directly compared with the calorimetric ones, represented in the upper panels of both figures by the derivative of the reversible part of the specific heat. As can be seen in Fig. 4(b) for the neat resin, in the glassy state the elastic intensity shows a decrease that can be attributed to the occurrence of vibrational processes and local motions taking place in a frozen environment, such as methyl group rotations. We note that the characteristic times of these localized processes are expected to be broadly distributed, due to the disorder inherent to the glassy state in addition to the effect of polydispersity in this particular sample. These motions have a clear signature in the inelastic intensity, leading to a pronounced maximum at approx. 200 K. In this temperature range, the average characteristic time of these motions matches the dynamic window explored in these scans. At higher temperatures, we observe an additional abrupt decrease of the elastic intensity for both Q-values investigated. This feature takes place close to the average calorimetric glass transition observed in this material. We note that there is no signature of the glass transition in the inelastic intensity. The dynamic processes leading to the additional decrease of the elastic intensity in this temperature range obviously present associated characteristic times very different from the nanosecond timescale probed by the inelastic scans. We expect that inelastic contributions of the α-relaxation processes (associated to the vitrification phenomenon) with energies ~2μeV would be present at higher temperatures than those here investigated.

In the case of the hydrogens in the resin component *within the blend* –as it is probed by neutrons on the labelled mixture at the two Q-values shown in Fig. 5— we observe that the additional decay of the elastic intensity with respect to the glassy behaviour takes place at a much lower temperature than in the pure resin. In fact, it occurs, within the uncertainties, at the (initial) glass-transition temperature as determined by DSC on the blend sample. This implies that, despite the huge difference in intrinsic mobilities of the two components, the atomic motions of the resin component become 'liquid-like' at the temperature dictated by the fast majority blend component, SBR. Thus, we can say that the minority resin molecules are 'animated' by the surrounding mobile environment imposed by the SBR

chains. A similar result has recently been observed on mixtures of SBR and PS-oligomers of 500 g/mol [23].

We note the occurrence of an additional decrease of the elastic intensity in the blend at higher temperatures (approx. 280 K). Actually, it coincides with the calorimetric glass transition of the pure resin. This coincidence could suggest the assignment of this new feature in the elastic scan to the existence of a second glass transition in the blend, attributable to 'dynamically immiscible' resin molecules within the mixture.

However, we observe that this extra-decrease of the elastic intensity corresponding to the resin in the blend occurs simultaneously with an increase of the inelastic intensity of this sample with respect to the pure resin behaviour (compare Fig. 5(c) and 4(c)). This observation suggests that in this temperature range the scattering function of the H-atoms of the resin within the blend has a width resolvable in the IN16B dynamic window, being thus detected as a quasielastic broadening of the signal. This implies an increase of the scattering at the considered energy transfer of 2μeV accompanied by a decrease of the elastic intensity. Thus, the finding of this effect in the neighbourhood of the pure resins' T_g could be just a mere coincidence. Nevertheless, we cannot completely discard that there are still degrees of freedom that were blocked at lower temperatures that become active at the pure resins' T_g. Actually, the apparent Q-insensitivity in the IFWS could also suggest the origin of this high-temperature increase to be due to local rotational motions. This hypothesis is rather speculative, since the peak is out of the range of the temperature scan performed.

4 Conclusions

EFWS provide a very sensitive tool to determine the onset of motions characteristic for the supercooloed liquid state. In the pure resin, we have found that the microscopic fingerprint of the glass transition revealed by the EFWS coincides very well with the glass transition temperature as determined by calorimetry. When blended with a polymer with a much lower glass-transition temperature, the resin shows its 'microscopic' glass transition signature close to the initial glass transition temperature of the whole sample as determined by calorimetry. These experiments provide the microscopic proof of 'animation' effects on the molecular motions of rigid molecules by the surrounding mobile environment imposed by the majority blend component in a mixture of industrial interest. Whether this effect is particular for systems where the slow component molecules are much smaller in size and highly polydisperse than the fast component is a question that shall be elucidated in future works.

We acknowledge the Grant PID2021-123438NB-I00 funded by MCIN/AEI/10.13039/501100011033 and by "ERDF A way of making Europe". We also acknowledge financial support of Eusko Jaurlaritza, code: and IT1566-22, as well as from the IKUR Strategy under the collaboration agreement between Ikerbasque Foundation and the Materials Physics Center on behalf of the Department of Education of the Basque Government.

References

1. J. Colmenero, A. Arbe, Soft Matter **3**, 1474-1485 (2007)
2. A. Zetsche, E.W. Fischer, Acta Polymerica **45**, 168-175 (1991)
3. G. Katana, E.W. Fischer, T. Hack, V. Abetz, F. Kremer, Macromolecules **28**, 2714-2722 (1995)
4. T.P. Lodge, T.C.B. McLeish, Macromolecules **33**, 5278-5284 (2000)
5. S. Shenogin, R. Kant, R.H. Colby, S.K. Kumar, Macromolecules **40**, 5767-5775 (2007)
6. T. Gambino, N. Shafqat, A. Alegría, N. Malicki, S. Dronet, A. Radulescu, K. Nemkovski, A. Arbe, J. Colmenero, Macromolecules **53**, 7020-7160 (2020)
7. T. Gambino, A. Alegría, A. Arbe, J. Colmenero, N. Malicki, S. Dronet, Polymer **187**, 122051 (2020)
8. N. Shafqat, A. Alegría, A. Arbe, N. Malicki, S. Dronet, L. Porcar, J. Colmenero, Macromolecules **55**, 7614-7625 (2022)
9. Y. Miwa, K. Usami, K. Yamamoto, M. Sakaguchi, M. Sakai, S. Shimada, Macromolecules **38**, 2355-2361 (2005)
10. D. Herrera, J.C. Zamora, A. Bello, M. Grimau, E. Laredo, A.J. Muller, T.P. Lodge, Macromolecules **38**, 5109-5117 (2005)
11. S. Arrese-Igor, A. Alegría, J. Colmenero, Macromolecules **43** 6406 (2010)
12. A.C. Genix, A. Arbe, F. Alvarez, J. Colmenero, L. Willner, D. Richter, Phys. Rev. E **72**, 031808 (2007)
13. M. Tyagi, A. Arbe, J. Colmenero, B. Frick, R. Stewart, Macromolecules **39**, 3007-3018 (2006)
14. A.C. Genix, A. Arbe, S. Arrese-Igor, J. Colmenero, D. Richter, B. Frick, P.P. Deen, J. Chem. Phys. **128**, 184901 (2008)
15. C. Lorthioir, A. Alegría, J. Colmenero, Phys. Rev. E **68**, 031805 (2003)
16. A. Bouty, L. Petitjean, J. Chatard, R. Matmour, C. Degrandcourt, R. Schweins, F. Meneau, P. Kwasniewski, F. Boue, M. Couty, J. Jestin, Faraday Discuss. **186**, 325−343 (2016)
17. A. Arbe, M. Appel, J. Colmenero, B. Frick, J. Maiz, L. Mangin-Thro, A. Mendia, J. Ollivier, J.A. Pomposo, N. Shafqat, Institut Laue-Langevin ILL (2019) ; https://doi.ill.fr/10.5291/ILL-DATA.9-11-1901
18. D. Bhowmick, J.A. Pomposo, F. Juranyi, V. García-Sakai, M. Zamponi, Y. Su, A. Arbe, J. Colmenero, Macromolecules **47**, 304-315 (2014)
19. D. Bhowmick, J.A. Pomposo, F. Juranyi, V. García-Sakai, M. Zamponi, Y. Su, A. Arbe, J. Colmenero, Macromolecules **47**, 3005-3016 (2014)
20. M. Gordon, J. S. Taylor, J. Appl. Chem. **2**, 493 -500 (1952)
21. S.W. Lovesey, *Theory of Neutron Scattering from Condensed Matter*, Clarendon Press: Oxford (1997)

22. J.S. Higgins, H.C. Benoit, *Polymers and Neutron Scattering*, University Press: Oxford (1997)
23. N. Shafqat, A. Alegría, N. Malicki, S. Dronet, F. Natali, L. Mangin-Thro, L. Porcar, A. Arbe, J. Colmenero (in progress)